

ABSTRACT

BASS, BRENDON STUART. Validating the Arcam EBM Process as an Alternative Fabrication Method for Titanium-6Al-4V Alloys. (Under the direction of Dr. Jerome Cuomo.)

The purpose of this work has been to show that Ti-6Al-4V alloys produced using the Arcam EBM process meet all the necessary requirements stated in AMS 4999 and other Ti-6Al-4V specifications. Ti-6Al-4V samples were fabricated using the Arcam EBM process and their microstructural and mechanical properties were evaluated using optical microscopy, scanning electron microscopy, tensile testing, hardness testing, and fracture testing. The results of these tests showed that, in general, the Arcam EBM produced samples were satisfactory.

Validating the Arcam EBM Process as an Alternative Fabrication Method for Titanium-6Al-4V Alloys

by
Brendon Stuart Bass

A thesis submitted to the Graduate Faculty of
North Carolina State University
in partial fulfillment of the
requirements for the Degree of
Master of Science

Materials Science and Engineering

Raleigh, North Carolina

2007

APPROVED BY:

Denis Cormier

Carl Koch

Jerome Cuomo
Chair of Advisory Committee

BIOGRAPHY

Brendon Bass was born on July 29, 1983 and raised in Nashville, North Carolina. He received his B.S. in Materials Science and Engineering from NCSU in 2005.

TABLE OF CONENTS

LIST OF TABLES	iv
LIST OF FIGURES	v
Chapter 1: Background	1
1.1 The Arcam EBM Process	1
1.2 Unconventional Machining Processes	2
1.2.1 Basic Fundamentals of Electron Beam Machining	2
1.2.2 Basic Fundamentals of Laser Beam Machining	4
1.3 Ti-6Al-4V Alloy	4
References	6
Chapter 2: Introduction	7
2.1 Microstructure	7
2.2 Mechanical Properties	10
2.3 Fabrication	10
2.4 Fracture Mechanics	13
2.5 Analysis Techniques	16
References	17
Chapter 3: Research	18
3.1 Sample Fabrication	18
3.2 Powder Fabrication	20
3.3 Microstructure	21
3.4 Mechanical Testing	30
3.4.1 Tensile Testing	30
3.4.2 Hardness	36
3.4.3 Fracture Toughness	37
3.5 Fractography	38
3.6 Improvement of Microstructural and Mechanical Properties	41
3.6.1 Varying the Process Parameters of the Arcam EBM Machine	41
3.6.2 HIP and/or Heat Treating at Various Times and Temperatures	44
3.6.3 Varying the Morphologies and Sizes of the Powder Alloy	47
References	49
Chapter 4: Conclusion	50

LIST OF TABLES

Table 3.1: Tensile Mechanical Properties of Ti-6Al-4V Specimens Fabricated Using the Arcam EBM Process.....	31
Table 3.2: Comparison of the Average Values of Selected Mechanical Tensile Test Parameters from Arcam EBM Fabricated Ti-6Al-4V Alloys to Various Aerospace Material Specifications for the Ti-6Al-4V Alloys Produced Using Already Established Methods.....	34
Table 3.3: Average Hardness Values for Arcam EBM Produced Ti-6Al-4V Specimens Compared to a Typical Ti-6Al-4V Alloy.....	36

LIST OF FIGURES

Figure 2.1: Schematic pseudo-binary phase diagram for Ti-6Al alloy with additions of Vanadium.....	7
Figure 2.2: The three basic modes of fracture.....	15
Figure 3.1: ASTM E8 Tensile Specimen Geometry.....	18
Figure 3.2: The three distinct surfaces of the tensile specimens.....	18
Figure 3.3: The build orientations of the Arcam EBM fabricated Ti-6Al-4V samples with respect to the start plate.....	19
Figure 3.4: The three, distinct solid-liquid growth planes; each growth plane is shaded for the three build orientations.....	20
Figure 3.5: Ti-6Al-4V gas atomized powder.....	21
Figure 3.6: Optical micrograph of an Arcam EBM fabricated Ti-6Al-4V alloy showing the two phase α (HCP)/ β (BCC) microstructure.....	22
Figure 3.7: A SEM micrograph showing the morphology and distribution of the β (BCC) phase in a EBM fabricated Ti-6Al-4V alloy.....	23
Figure 3.8: Optical micrograph of an Arcam EBM fabricated Ti-6Al-4V alloy showing the columnar grains normal to the planar solid-liquid growth interface.....	24
Figure 3.9: XY oriented sample showing columnar grains aligned perpendicular to the planar solid-liquid growth interface.....	25
Figure 3.10: Face plane of XY build oriented sample showing the cross-section of the columnar grains.....	26
Figure 3.11: Columnar grains of the (A) face plane and (B) cross-section plane of the YZ build orientation.....	27
Figure 3.12: Columnar grains of the (A) face plane and (B) edge plane of the XZ build orientation.....	28
Figure 3.13: Micrographs showing the cross-sections of columnar grains for (A) a XZ cross-section plane and (B) a YZ edge plane.....	29

Figure 3.14: Comparison of Average Tensile Mechanical Properties for the Three Different Build Orientations.....	32
Figure 3.15: Comparison of the Average Values of Selected Mechanical Tensile Test Parameters from Arcam EBM Fabricated Ti-6Al-4V Alloys to Various Aerospace Material Specifications for the Ti-6Al-4V Alloys Produced Using Already Established Methods.....	35
Figure 3.16: Fracture Toughness Values for Horizontally and Vertically Oriented Arcam EBM Fabricated Ti-6Al-4V Specimens.....	37
Figure 3.17: SEM Fractographs of Arcam EBM produced Ti-6Al-4V Tensile Specimens.....	39
Figure 3.18: Raster pattern used in Arcam EBM process.....	43

Chapter 1: Background

1.1 The Arcam EBM Process

In industry today, there is a great demand for rapid manufacturing processes that allow parts to be made quickly and with low tooling costs. Current forging and cast technologies are time consuming processes that require the use of expensive tooling methods that often leave much of the original material wasted as scrap. Also, current manufacturing methods simply are not capable of producing complex parts that some industrial applications require. The Arcam Electron Beam Melting (EBM) process was developed as a way to avoid these problems that arise with traditional manufacturing methods.

The Arcam EBM process is at the forefront of the Solid Free Form Fabrication Industry, providing a revolutionary method of part manufacturing. As described on their website, the Arcam EBM S12 is a machine developed using Arcam's Computer Automated Design (CAD) to metal technology that allows for solid metal components to be created directly from a CAD model, thereby greatly reducing lead times for parts. This direct manufacturing process also eliminates the need for mass produced tooling. The Arcam EBM process also allows for intricate geometries with dimensions as small as a millimeter. The fundamental idea behind this technology is to build up metal parts in layers of metal powder in which each layer (about 100 μm thick) is melted by an electron beam, at a velocity of approximately 500 mm/sec, to achieve the geometry defined by the computer model⁽¹⁾. The EBM process provides high power (up to 4.8 kW) to fully melt the metal powder. This process is done in a

vacuum with a pressure of 10^{-6} mbar at the electron gun and a pressure of 10^{-3} mbar in the chamber to create a clear path for the electron to travel to the metal. The vacuum also provides a clean environment to help minimize contamination and also a good thermal environment to allow for good form stability and controlled thermal balance in the part. The result is a direct manufactured part that is able to meet strict strength and material requirements. Final machining can easily be done with conventional methods such as high speed milling, grinding, and turning ⁽²⁾.

There are other methods of free form fabrication (FFF) that exist ⁽²⁾, but do not offer the same functionality as the Arcam EBM process. Most other FFF techniques deal with plastic or paper. The techniques that do use metal, such as those involving laser beams, are based on sintering methods that do not allow the same degree of freedom in regards to material selection and properties as the Arcam EBM process. Sintering methods also require certain binding agents in the metal powder, whereas the Arcam EBM process does not. These advantages make the Arcam EBM process stand out from the competition ⁽²⁾.

1.2 Unconventional Machining Processes

1.2.1 Basic Fundamentals of Electron Beam Machining

In conventional electron beam machining, a stream of high velocity electrons bombard the specimen surface. The kinetic energy of the electrons is transferred to the specimen, producing intense focused heat that can melt and/or vaporize the specimen material ⁽³⁾. Very

high velocities can be reached by using enough voltage; for example, an accelerating voltage of 150,000 V can create an electron velocity of 228,478 km/sec⁽³⁾. Because an electron beam can be focused to a point having a diameter ranging from 10-200 μm , a power density of 6500 W/mm² is capable of being reached. In an electron beam machine, the electrons are emitted from a cathode, made of a hot tungsten filament. A grid cup is used to shape the beam, and the electrons are accelerated by the large potential difference between the cathode and the anode, which is the material to be machined. The beam is focused using electromagnetic lenses. To control the beam movement, magnetic deflecting coils are used. In order to prevent collision of the accelerating electrons with air molecules, the machining is performed in a vacuum (around 10⁻⁵ Torr)⁽³⁾. Since the energy density is extremely high, the specimen material 25-50 μm away from the electron beam remains at the room temperature. Using electron beam machining, a maximum material removal rate of 10 mm³/min can be achieved. An advantage of electron beam machining is that it can be used on all materials; however use of the process is limited due to its consumption of very high specific energy, the need for a vacuum, and machine cost⁽³⁾.

The Arcam EBM process incorporates the basics of electron beam machining in its technique. Instead of using the electron beam to shape the final dimensions of a part or to melt an alloy for refinement purposes, the Arcam EBM process uses it to melt and solidify powder into a near net shape part.

1.2.2 Basic Fundamentals of Laser Beam Machining

Laser beam machining involves using a highly coherent beam of electromagnetic radiation having wavelengths that vary from 0.4 to 0.6 μm and capable of producing a power density up to 10^7 W/mm^2 . Laser beam machining consists of three phases: interaction of laser beam with the material, heat conduction and temperature rise, and melting, vaporization, and ablation. The absorbed light travels into the material and its energy gradually transfers into the lattice atoms as heat. Most of the energy is absorbed in a thin layer at the surface (typically around 0.01 μm). The efficiency of the laser beam machining is low, only around 0.3 to 0.5%. The normal output energy of a laser is 20 J having a one millisecond pulse duration. The peak power can reach a value of 20,000 W⁽³⁾. One advantage of laser beam machining over electron beam machining is that it can operate under normal atmosphere. However, laser beam machining requires very large power consumption (typically around 1000 W/mm³/min) and has a lower maximum material removal rate (5 mm³/min) than electron beam machining. Also, it can not be used on materials having a high heat conductivity or high reflectivity⁽³⁾.

1.3 Ti-6Al-4V Alloy

Research was conducted to compare the material properties and characteristics of the Arcam EBM process to traditional forging and casting techniques. The particular material of interest is the Ti-6Al-4V (6 wt% Al, 4 wt% V) alloy.

Ti-6Al-4V alloy is the most used titanium alloy in industry as a result of its good machinability and mechanical properties. It accounts for about 45% of total titanium

production worldwide ⁽⁴⁾. Its defining characteristics such as superior corrosion resistance, strength-to-weight ratio, and fatigue properties make it ideal for aerospace, automotive, and marine applications. Due to its biomedical capability, Ti-6Al-4V is also widely used in the medical industry for implants and prostheses. It can be readily welded, forged, and machined, and is available in many varieties of mill product forms such as wire, sheet, extrusions, and rod ⁽⁵⁾. This work will focus on evaluating the microstructure and mechanical properties of Ti-6Al-4V specimens produced using the Arcam EBM process and determining if this process is a viable alternative to previously established fabrication techniques.

References

1. D. Cormier et al. *Optimization of Electron Beam Melting Process*. IIE Annual Conference. 09C Rapid Prototyping III. 2004.
2. www.arcam.com.
3. A. Ghosh et al. *Manufacturing Science*. Ellis Horwood Limited. Chichester. 1986.
4. D. Betner et al. *Metals Handbook Ninth Edition: Volume 3 Properties and Selection: Stainless Steels, Tool Materials and Special-Purpose Metals*. American Society for Metals. USA. 1980.
5. W. Smith. *Structure and Properties of Engineering Alloys*. McGraw-Hill, Inc. USA. 1993.

Chapter 2: Introduction

2.1 Microstructure

Ti-6Al-4V is comprised of α and β phases with the α phase having a hexagonal close packed (HCP) crystal structure and the β phase having a body centered cubic (BCC) crystal structure. Aluminum is used as an α stabilizer as it increases the temperature at which the α phase is stable. Vanadium is used to give stability to the β phase at lower temperatures⁽¹⁾. The microstructure of the Ti-6Al-4V alloy depends mainly upon its processing history and thermal treatment. The microstructural changes due to thermal treatment of the Ti-6Al-4V alloy are most easily understood by observing the pseudo-binary Ti-6Al phase diagram shown in Figure 2.1.

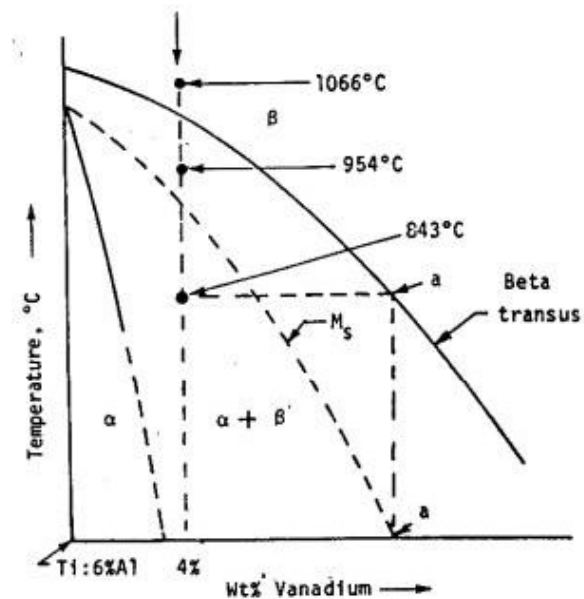


Figure 2.1: Schematic pseudo-binary phase diagram for Ti-6Al alloy with additions of Vanadium⁽²⁾.

The microstructure produced due to thermal treatments varies depending upon the temperature at which cooling begins and the cooling method used. The most common methods of cooling, in order of quench rate, are water quenching, air cooling, and furnace cooling.

Heating a Ti-6Al-4V specimen to 1066°C, which is above the β transus, and keeping it there for an hour produces a completely β -phase microstructure. Water quenching a specimen from 1066°C produces a microstructure consisting of all α' (titanium martensite). The microstructure of α' martensite is characterized by individual platelets which are heavily twinned and contain a HCP crystal structure. The grain refinement associated with the BCC to HCP transformation and the increased dislocation density due to the rapid transformation, strengthen the titanium martensite. Aging or tempering titanium martensite at certain temperatures causes precipitation of the β phase from the unstable α' martensite, which strengthens the alloy even further. Air cooling from 1066°C produces a microstructure made up of acicular α that is transformed from the β phase by means of nucleation and growth. Furnace cooling from 1066°C creates a microstructure that consists of coarse, plate-like α formed by nucleation and growth. Some β phase is retained intergranularly due to the slow cooling rate ⁽²⁾.

Heating a Ti-6Al-4V specimen to 954°C, which is below the β transus, produces a microstructure of primary α coexisting with the β phase. Water quenching the specimen to room temperature transforms the β phase to α' titanium martensite, thereby producing a

microstructure of primary α embedded in α' . Air cooling the specimen from 954°C produces a microstructure consisting of primary α in a transformed β matrix, some of which is acicular α . Furnace cooling the specimen from 954°C produces a microstructure of equiaxed α and intergranular unchanged β ⁽²⁾.

Heating a Ti-6Al-4V specimen to 843°C, just below the M_s temperature, produces a microstructure with a lot less β phase present than at the higher temperatures discussed previously. Water quenching the specimen from 843°C produces a microstructure consisting of primary α and unchanged β . The unchanged β is metastable, and may undergo an ensuing strain-induced transformation ⁽²⁾.

Forging a Ti-6Al-4V specimen also affects the resulting microstructure. A Ti-6Al-4V bar forged with a 75% reduction in area at 982°C, just below the β transus, and reheated 2 hours at 732°C followed by air cooling, produces a microstructure consisting of platelike as well as equiaxed α with small amounts of transformed β . Forging a similar bar with the same amount of area reduction, but at a lower temperature of 899°C produces a microstructure having fine elongated α - β . These results show that the microstructure becomes more elongated the lower the temperature of working below the β transus. If extensive hot working is done below the β transus, but above the recrystallization temperature, an equiaxed structure is produced ⁽²⁾.

2.2 Mechanical Properties

The tensile properties of Ti-6Al-4V alloys vary depending upon how it is processed. An annealed Ti-6Al-4V bar typically has an ultimate tensile strength (UTS) of 130 ksi and a yield strength (YS) of 120 ksi. It normally has a 10% elongation and a 20% reduction in area. A solution treated aged bar and forgings 1 to 2 in thick give an UTS of around 150 ksi, a YS of 140 ksi, 8% elongation, and 20% reduction in area. The hardness of Ti-6Al-4V ranges from 36 to 39 HRC. Ti-6Al-4V has a Poisson's ratio of 0.33 and an elastic modulus of 110 GPa in tension and 117 GPa in compression. At room temperature (25°C), an annealed plate of Ti-6Al-4V has a fracture toughness of about 68 ksi in^{1/2}, and a fracture toughness of 39 ksi in^{1/2} for a solution treated and aged sample ⁽³⁾.

2.3 Fabrication

The manufacturing of Ti-6Al-4V ingots into parts involves two steps: primary and secondary fabrication. Primary fabrication consists of all processes that convert ingots into general mill products such as billets, bars, plates, sheets, strips, extrusions, tubes and wires. Secondary fabrication deals with manufacturing processes that produce finished parts from mill products. These processes include die forging, extrusion, hot and cold forming, machining, joining, and chemical milling; each of which can strongly influence the properties of Ti-6Al-4V alloys. Since the Arcam EBM process only differs from regular forging and casting techniques during secondary fabrication, that is what will be discussed here.

Forging is a process in which metal is heated and shaped by plastic deformation using compressive force, usually in the form of a hammer or press. Die forging can be categorized into three groups: open-die forging, impression-die forging, and closed-die forging. Open-die forging permits free deformation of at least some of the workpiece surfaces. Impression-die forging yields much more constrained deformation, and closed-die forging gives completely constrained deformation. Open-die forgings produce workpieces of lesser accuracy than impression or closed-die forgings⁽⁴⁾. With die forging, a variety of shapes can be produced using relatively simple dies; however the process often requires a complex sequence of deformation steps. Impression and closed-die forging produces parts using complex die shapes, but require only a simplified sequence of deformation steps.

In the extrusion process, a workpiece is pushed against a deforming die while being supported against unrestrained deformation in a container. This process allows for the possibility of heavy deformations together with a wide array of extruded cross sections. There are two different types of extrusion: direct and indirect. In direct extrusion, the product emerges from the same direction as the movement of the punch meaning the workpiece experiences friction with container wall. In indirect extrusion, the product travels in the opposite direction of the punch. In this process, the workpiece is at rest and no friction occurs⁽⁴⁾.

Machining differs from forging and extrusion in that instead of plastically deforming a part, the desired shape is obtained by removing material in the form of chips. Machining can also

be used to improve the tolerances and surface finishes of previously made workpieces. One advantage of machining is that complex shapes, tolerances, and surface finishes can be created that are often unattainable by other processing techniques. The disadvantage to machining is that it removes material in the form of relatively small particles that are difficult to recycle and can become easily mixed. This material is usually wasted as scrap ⁽⁴⁾.

The joining process differs from the previously discussed processes in that it takes parts produced by other processes and combines them into a more intricate part. Permanent joining processes are divided into four categories: mechanical, solid-state, fusion, and liquid-solid. Mechanical joining uses mechanical fasteners such as rivets, stitches, staples, and seams to join two or more workpieces. Solid-state welding involves the formation of interatomic bonds by bringing the atoms of two surfaces close together. It consists of cold welding, diffusion pressure, hot welding, and friction welding. Fusion welding is when the interatomic bond is made by melting the base metals and filler (if necessary). Liquid-solid state bonding occurs when a filler metal is used to establish the joint. This process requires no melting of the base metal and the strength of the bond is derived from the adhesion between the filler and base metal. In liquid-solid state bonding (such as brazing and soldering) the strength of the joint is higher than the strength of the filler ⁽⁴⁾.

Chemical milling is a process that is used to remove pockets of material. An etchant is used to dissolve the material in all directions. Masks can be used to prevent the etchant from

dissolving certain parts of the material. This process is often used to create undercuts of a material to increase the stiffness of panels with capped ribs.

2.4 Fracture Mechanics

The understanding of how a material fractures gives key insight into the properties of the material. Every material can be categorized as ductile or brittle, or portraying qualities of both. Ultimately, the atomic bonding of the material is the determining factor in whether or not it is ductile or brittle. An ideally ductile failure is when the material necks down under tension in a continuously plastic manner until the narrowing neck becomes atomically sharp and the material splits apart. An ideally brittle fracture occurs when the material experiences a sudden and catastrophic fracture with no observable plastic flow either prior to or during failure⁽⁵⁾. Ductile fracture is caused by dislocations of the atomic bonds, while brittle fracture is caused by the creation of atomically sharp cleavage cracks. These cracks in a material can concentrate the applied stress to the area of the crack tip resulting in a magnified stress many orders of magnitude higher. Once this magnified stress at the crack tip surpasses the maximum atomic bond strength, the crack will propagate through the solid and fracture the material. Crack formation in materials occurs in a variety of ways by any mechanism that locally causes an adequately high stress. The condition of a materials free surface affects how easily a crack can form. A smooth surface will take longer to initiate a crack than a machined surface. For a smooth surface, crack initiation almost always starts at the free surface⁽⁶⁾. In the cases where crack initiation occurs in the interior, an internal free surface such as a void or an interface with a precipitate is the cause. These sites create holes that

form ahead of the main crack and are connected by shear bands. The shear bands also contain voids, but are normally much smaller than the holes they connect. The range of resolved shear stress leads to slip band formation that cracks within the grains whose orientation puts the preferred shear planes along the maximum shear directions (45° to the applied stress). These slip bands migrate to the free surfaces of the material and cause fracture. The ability of a crack to emit dislocations depends on its atomic structure, and the type of bonding at the crack determines whether external chemicals can interact with the crack in an embrittling fashion.

A crack consists of two steps, an initial cut made in the material, creating the cleavage plane, and forces exerted on the free surfaces of the material which specify the particular fracture mode. The three basic fracture modes are shown in Figure 2.2.

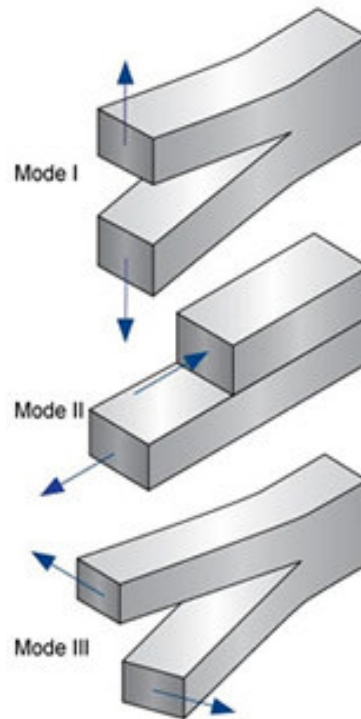


Figure 2.2: The three basic modes of fracture⁽⁷⁾.

Mode I shows a tensile stress with the principle stress axis normal to the cleavage plane. This mode is the only mode that leads to a physical fracture because it is the only mode whose external stress physically separates the two surfaces on the cleavage plane; without this separation, rewelding would take place even after the stress is applied. Mode II shows a stress that is a shear parallel to the cut in the plane direction, while mode III shows a stress that is a shear parallel to the cut in the antiplane direction⁽⁵⁾. It is important to note that most actual cracks are not pure cases. The crack fronts are not normally straight and the fracture surfaces are not usually flat; thus it is possible that a crack may be produced which is mainly mode II or III, but exhibits enough of mode I to separate the cleavage plane.

2.5 Analysis Techniques

Several techniques were used in the evaluation of Ti-6Al-4V specimens produced by the Arcam EBM S12. To evaluate the strength and ductility of the specimens, a 220-kip MTS closed-loop universal testing machine was used to tensile test the samples. Fractography and microscopy analysis were conducted using a JEOL 6400F Field Emission SEM, a Zeiss Stemi 2000-C optical microscope, and a Zeiss Axiovert 40 MAT optical microscope. For the machining of the samples final dimensions, a Cincinnati Milacron CNC milling machine was used. Fracture toughness testing was conducted using a Fatigue Dynamics three-point bend machine for the crack initiation, and a RSL four-point bend machine to break the samples. Macro-hardness tests were carried out using a Wilson Rockwell hardness tester.

References

1. R. Boyer. *Metals Handbook Ninth Edition: Volume 9 Metallography and Microstructures*. American Society for Metals. USA. 1985.
2. W. Smith. *Structure and Properties of Engineering Alloys*. McGraw-Hill, Inc. USA. 1993.
3. D. Betner et al. *Metals Handbook Ninth Edition: Volume 3 Properties and Selection: Stainless Steels, Tool Materials and Special-Purpose Metals*. American Society for Metals. USA. 1980.
4. J. Schey. *Introduction to Manufacturing Processes*. McGraw-Hill, Inc. USA. 2000.
5. R. Thomson et al. *Fundamentals of Fracture: IV Cracking and Failure Mechanisms*.
6. R. Sanford. *Principles of Fracture Mechanics*. Pearson Education, Inc. USA. 2003.
7. www.ndt-ed.org.

Chapter 3: Research

3.1 Sample Fabrication

Ti-6Al-4V samples were created from CAD models corresponding to the geometry given in the ASTM E8 tensile coupon specification, as shown in Figure 3.1.

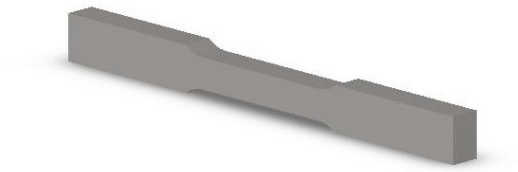


Figure 3.1: ASTM E8 Tensile Specimen Geometry

The three distinct surfaces on the tensile coupons were labeled as follows: face plane, edge plane, and cross-section plane, as shown in Figure 3.2.

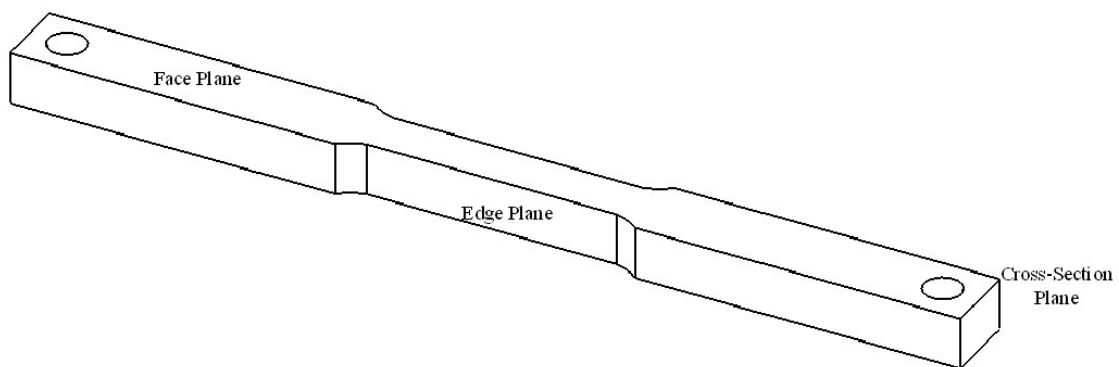


Figure 3.2: The three distinct surfaces of the tensile specimens

In order to evaluate the effect of sample orientation on the mechanical properties, samples were built in three different orientations: standing up, laying down flat, and lying on the side.

Figure 3.3 shows the build orientations of the samples with respect to the start plate.

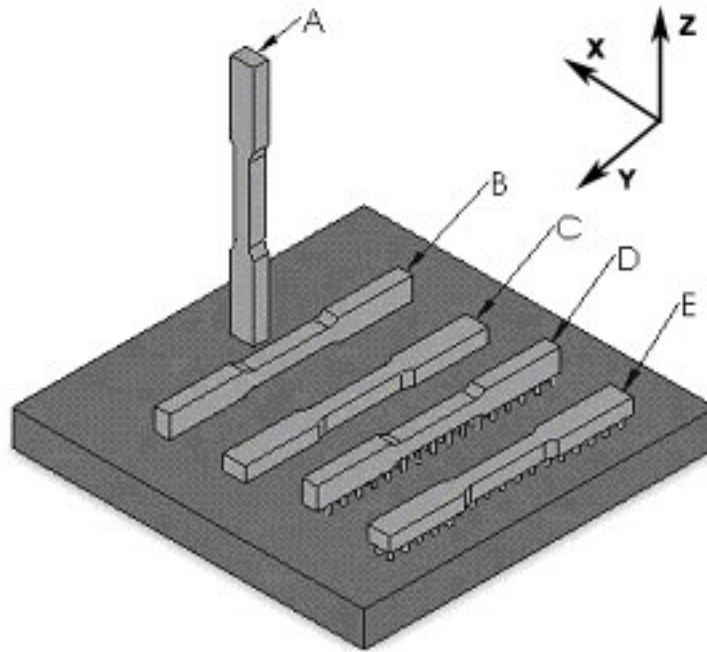


Figure 3.3: The build orientations of the Arcam EBM fabricated Ti-6Al-4V samples with respect to the start plate

Samples built in the orientation shown in specimen A were labeled “XZ,” while samples built in the orientations B and C were labeled “YZ” and “XY,” respectively. Each of these three build orientations has a unique solid-liquid growth interface oriented in the “Z” direction as shown in Figure 3.4. Build orientations D and E will be discussed later.

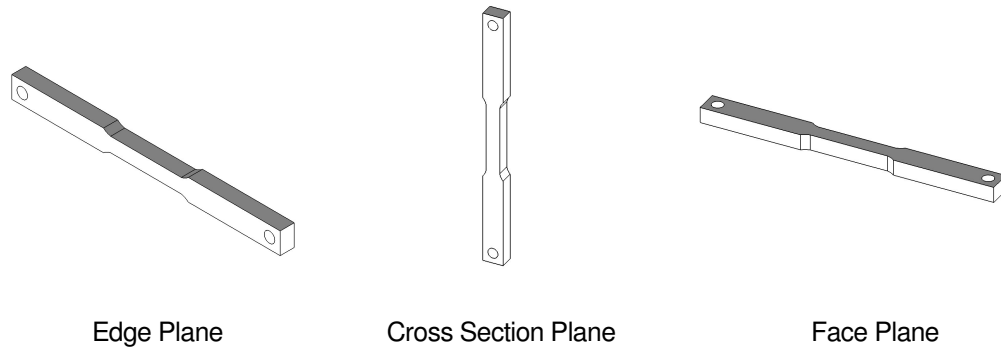


Figure 3.4: The three, distinct solid-liquid growth planes; each growth plane is shaded for the three build orientations.

3.2 Powder Fabrication

All the samples fabricated in this research came from gas atomized Ti-6Al-4V powder (except the fracture toughness samples, see Section 3.4.3). Gas atomization is a process that involves liquid metal being separated into fine droplets that freeze rapidly before they come in contact with each other or a solid surface. These fine droplets are created by high energy jets of gas that impact the thin stream of liquid metal causing it to disintegrate. The resultant powder is spherical/globular in shape without any internal porosity⁽¹⁾. Figure 3.5 shows the typical morphology of Ti-6Al-4V gas atomized powder. The powder used in this work ranged from 44 to 149 μm in size.

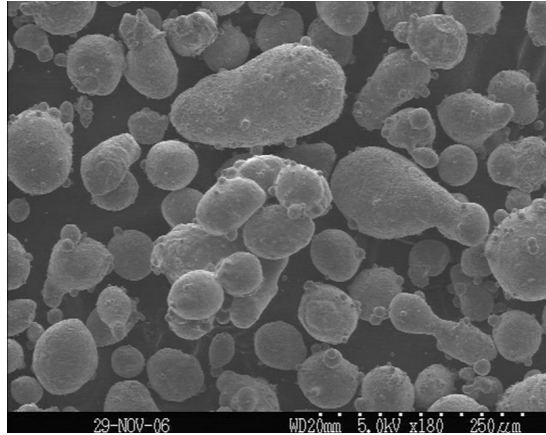


Figure 3.5: Ti-6Al-4V gas atomized powder.

3.3 Microstructure

The Ti-6Al-4V specimens made using the Arcam EBM process were polished and etched for microstructural analysis. The grinding and polishing sequence was as follows: 60, 120, 240, 320, 400, 600, 800, and 1200 grit, followed by 1.0 micron and 0.3 micron alumina. There were several etchants used to bring out the various aspects of the microstructure. Kroll's reagent (3mL HF, 5mL HNO₃, and 100mL H₂O) was found to work well as an overall etchant since it brought out the matrix and grain boundaries in the microstructure. Keller's reagent (2mL HF, 3mL HCl, 5mL HNO₃, and 190mL H₂O) also worked well as an overall etchant when followed with a post etchant consisting of 1 mL HF, 2mL HNO₃, 50mL H₂O₂, and 47mL H₂O. An etchant consisting of 10mL HF, 5mL HNO₃, and 85mL H₂O proved to work well at bringing out the grain boundaries, while an etchant consisting of 6g NaOH, 16mL H₂O, and 10mL H₂O₂ was found to work well at showing the matrix of the microstructure.

Micrographs taken of the Ti-6Al-4V specimens clearly show both the α (HCP) and β (BCC) phases present in the microstructure. The α (HCP) phase appears white and the β (BCC) appears black in the microstructure shown in Figure 3.6.

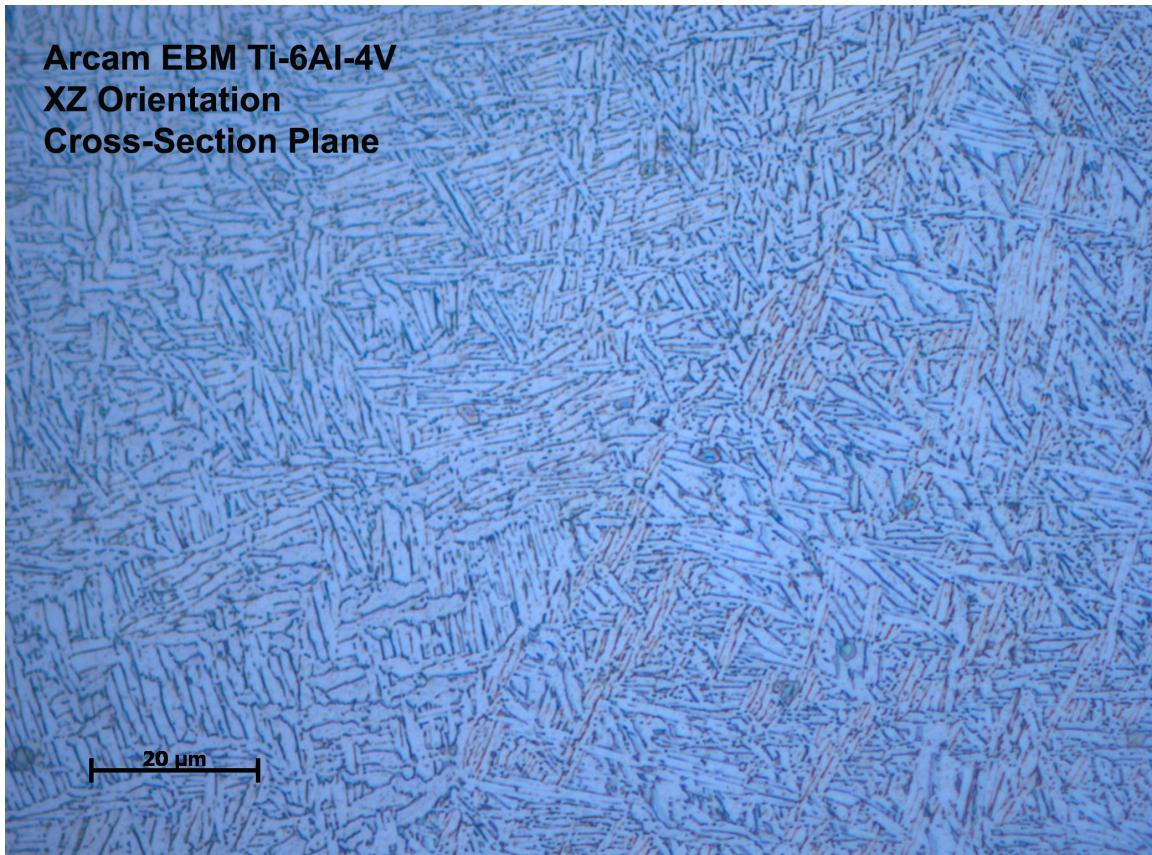


Figure 3.6: Optical micrograph of an Arcam EBM fabricated Ti-6Al-4V alloy showing the two phase α (HCP)/ β (BCC) microstructure.

As displayed in Figure 3.6, the α (HCP) phase has an acicular or plate-like morphology. This type of α (HCP) morphology is common among many α/β titanium alloys, especially those that have been cooled from the β region⁽²⁾ and as discussed previously in Chapter 2.1. The β (BCC) phase in Figure 3.6 appears to be located primarily in between the α phase entities, with some β particles spread throughout the microstructure.

The β (BCC) phase is shown much clearer when using a scanning electron microscope (SEM). Figure 3.7 is a SEM micrograph that shows the β (BCC) phase with better resolution.

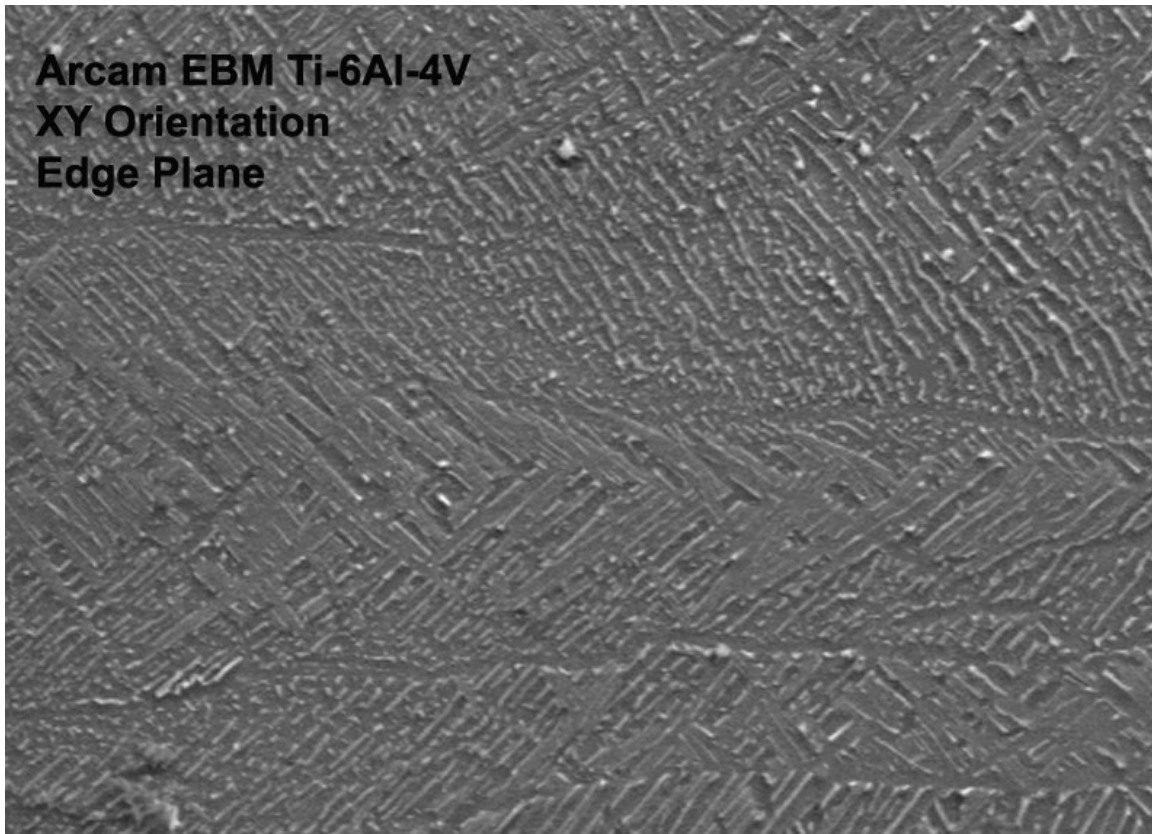


Figure 3.7: A SEM micrograph showing the morphology and distribution of the β (BCC) phase in a EBM fabricated Ti-6Al-4V alloy.

One microstructural characteristic that was prevalent in all three build orientation samples was the presence of columnar boundaries. These columns were aligned normal to the planar solid-liquid growth interface. The columns contained the two phase α/β mixture with the α (HCP) phase appearing to have preferred orientations within the columnar structures. Due to this change in the α (HCP) orientation between the columnar structures, along with the fact that a columnar grain structure is observed in many types of metal castings and some laser

fabricated metals under certain conditions⁽³⁾, it is reasonable to assume that the columnar boundaries found in these specimens represent grain boundaries. An example of the columnar structure found in these specimens is shown in Figure 3.8.

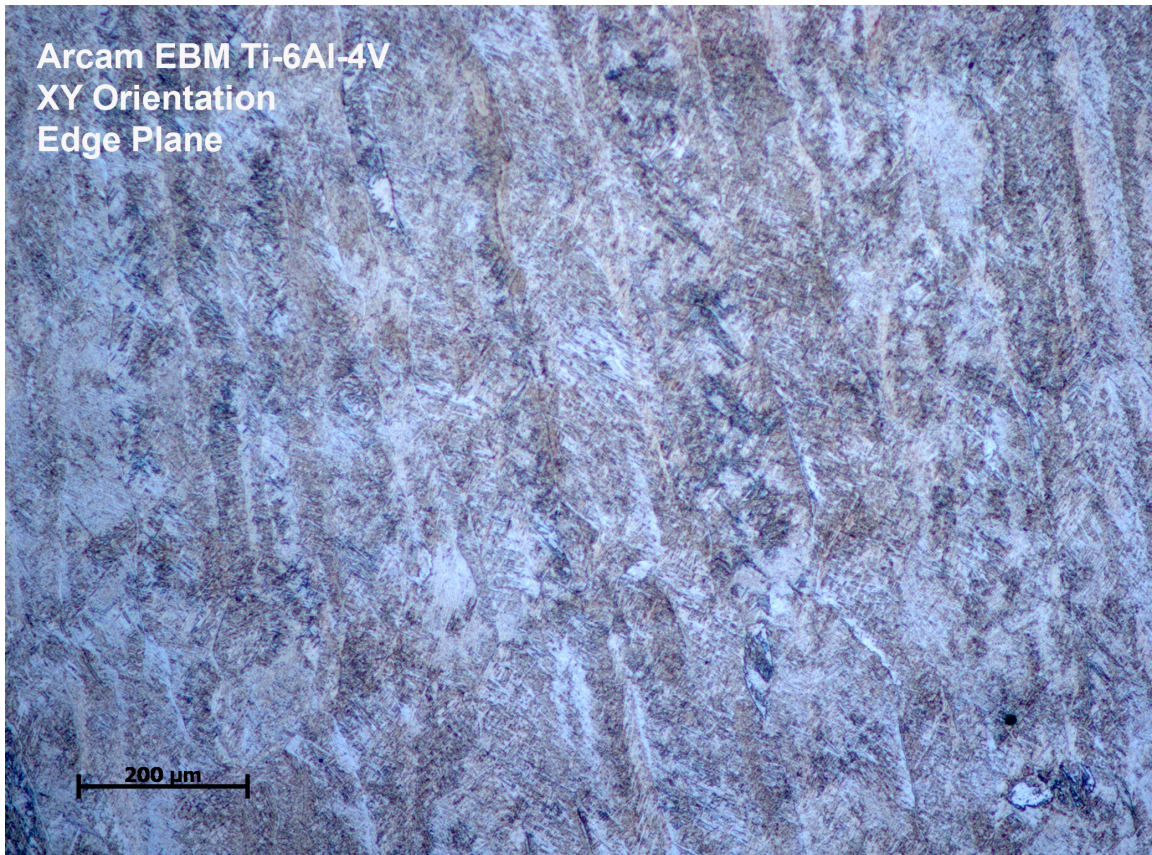


Figure 3.8: Optical micrograph of an Arcam EBM fabricated Ti-6Al-4V alloy showing the columnar grains normal to the planar solid-liquid growth interface.

In the figure above, the micrograph is of the edge plane of a XY build orientation sample.

The planar solid-liquid growth interface for XY oriented samples is the face plane; therefore the columnar grains shown in Figure 3.8 are aligned perpendicular to this plane. The cross-section plane of a XY oriented sample is shown in Figure 3.9. As expected, this figure shows the columnar grains aligned perpendicular to the planar solid-liquid growth interface as well.

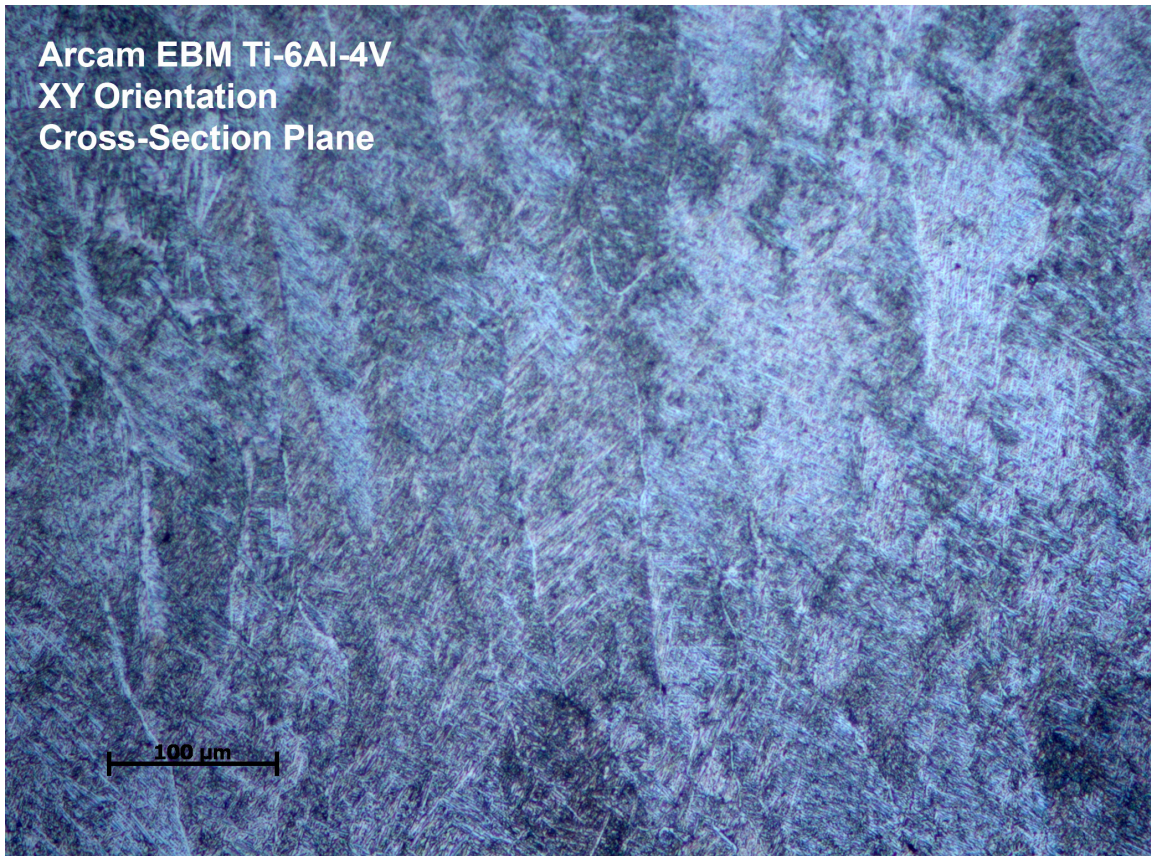


Figure 3.9: XY oriented sample showing columnar grains aligned perpendicular to the planar solid-liquid growth interface.

Since the face plane is the planar solid-liquid growth plane of the XY build oriented samples, the microstructure should show the cross-section of the columnar grains. Figure 3.10 proves this claim.

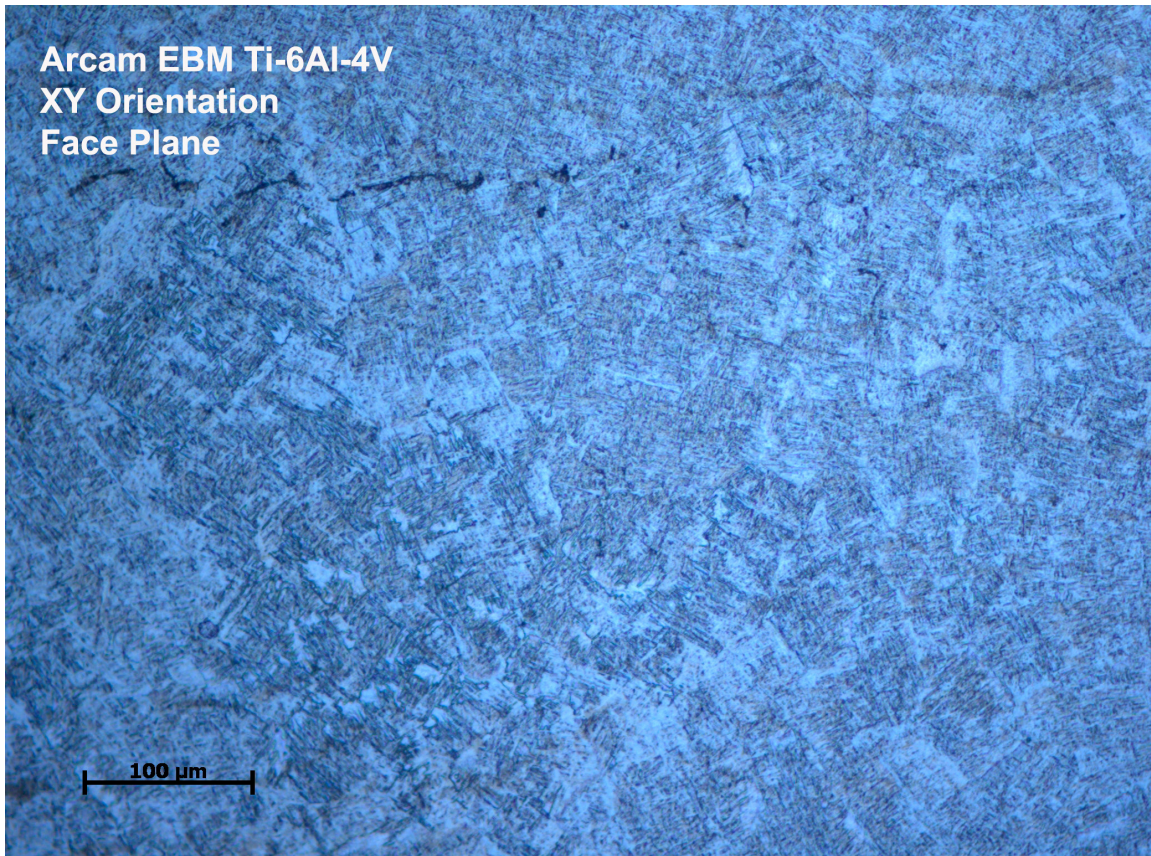
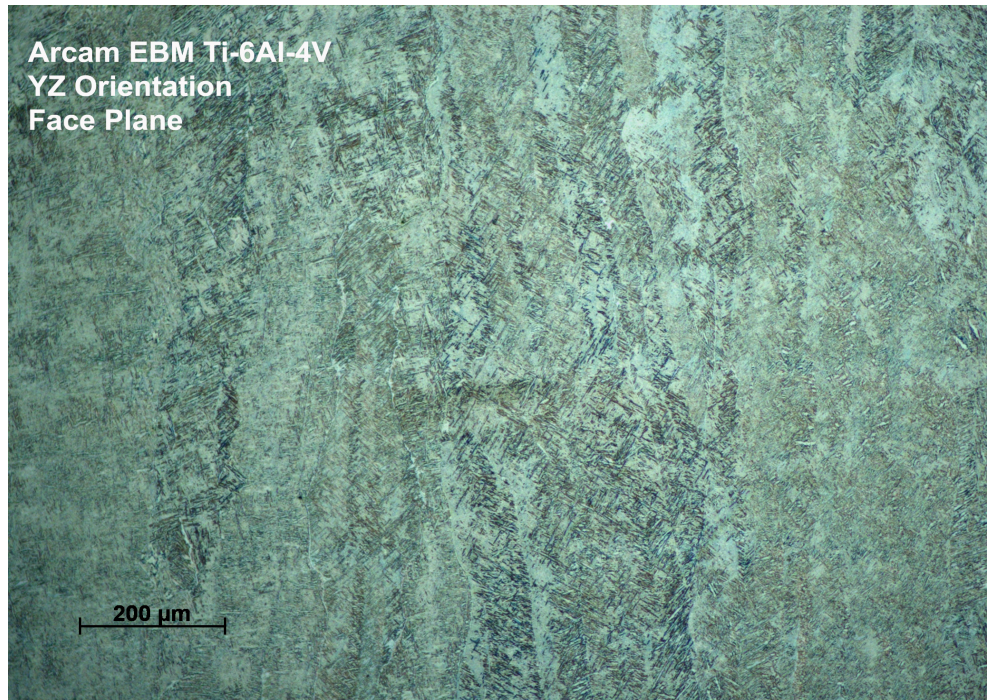
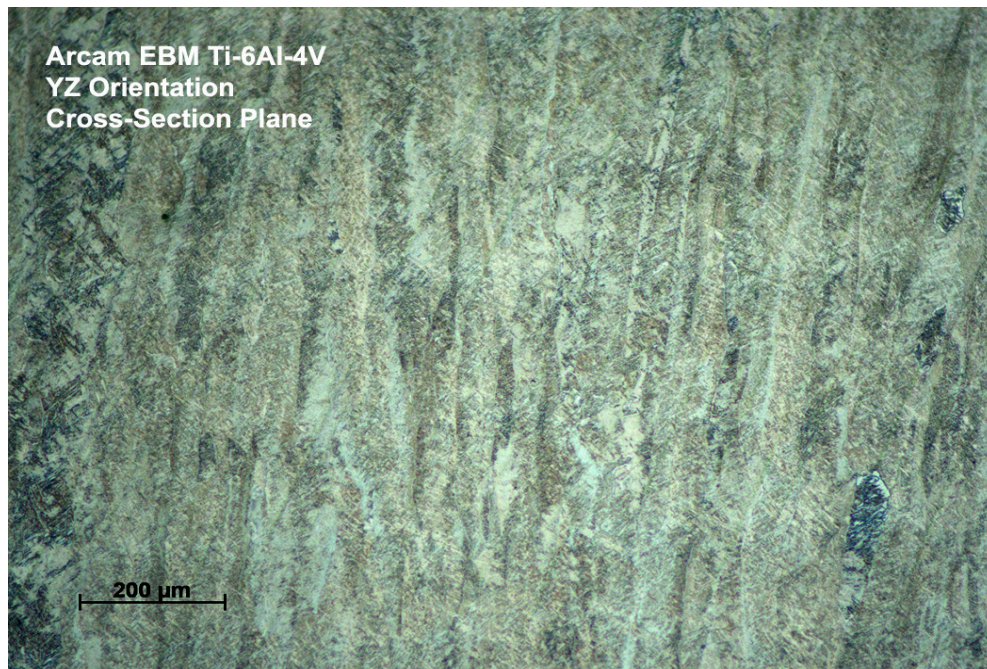


Figure 3.10: Face plane of XY build oriented sample showing the cross-section of the columnar grains.

As previously mentioned, the presence of the columnar grain boundaries aligned perpendicular to the planar solid-liquid growth plane is observed in all three build orientations. This means that the face plane and cross-section plane for the YZ build orientation should exhibit columnar grains, as well as the face plane and edge plane for the XZ build orientation. These columnar grains are shown in Figure 3.11 a and b, and Figure 3.12 a and b, respectively.

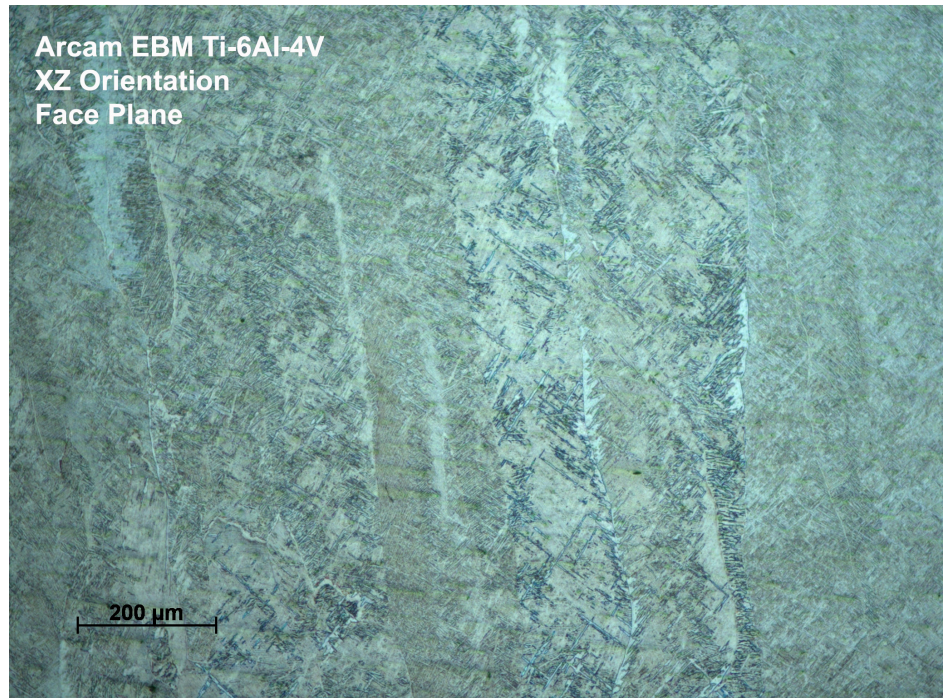


(A)

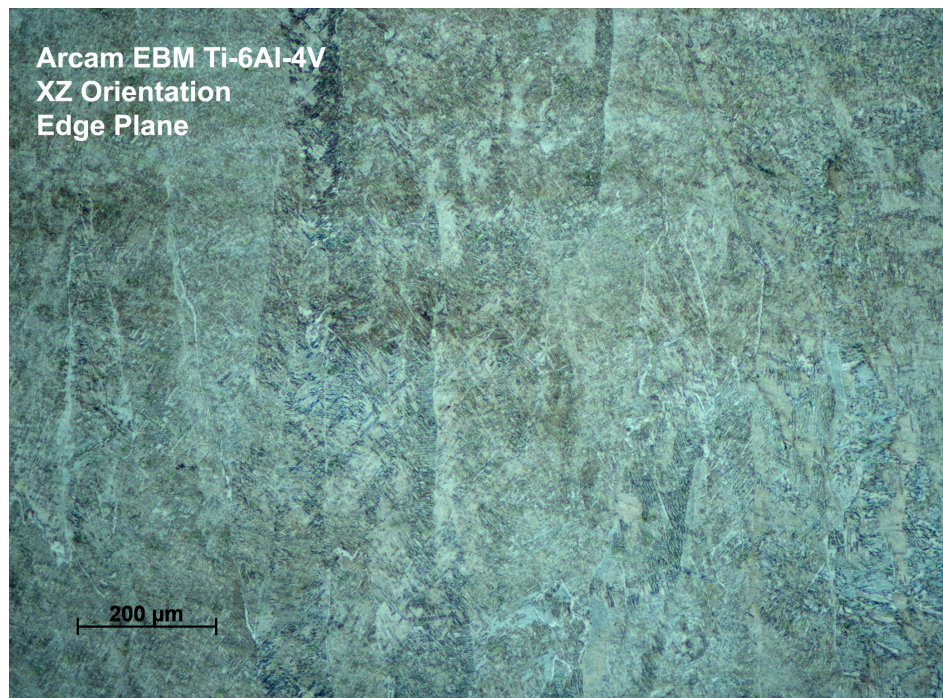


(B)

Figure 3.11: Columnar grains of the (A) face plane and (B) cross-section plane of the YZ build orientation.



(A)



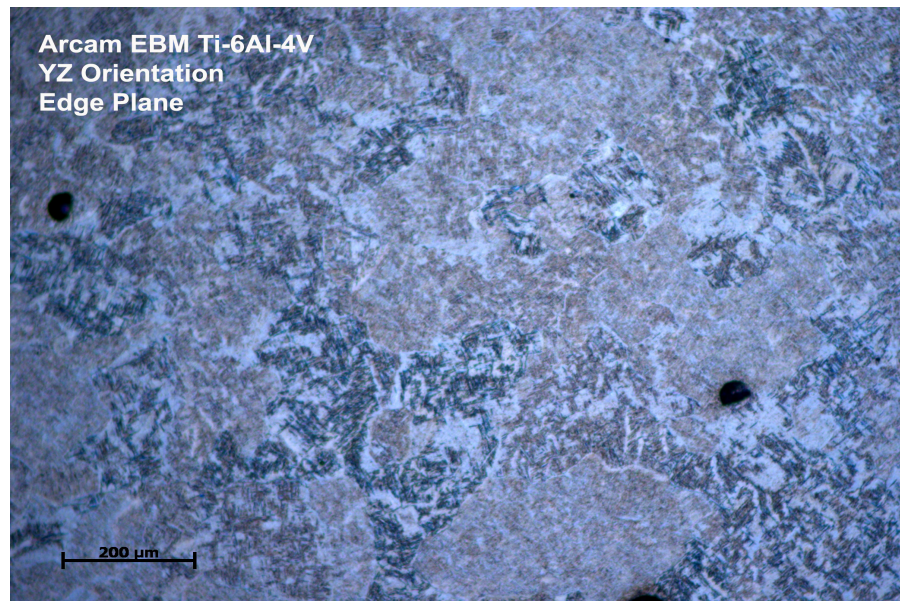
(B)

Figure 3.12: Columnar grains of the (A) face plane and (B) edge plane of the XZ build orientation.

As it was with the XY build orientation, the cross-sections of the columnar grains for the YZ and XZ build orientations were also present on the planar solid-liquid growth planes, as shown in Figure 3.13 a and b.



(A)



(B)

Figure 3.13: Micrographs showing the cross-sections of columnar grains for (A) a XZ cross-section plane and (B) a YZ edge plane.

As seen in the above figures, the diameters of the columnar grains' cross-sections range from about 100 to 200 μm . The lengths of the columnar grains tend to run the entire span of the specimens.

3.4 Mechanical Testing

The mechanical properties of the Arcam EBM fabricated Ti-6Al-4V alloys from each of the three build orientations were established. Tensile testing was performed to determine the UTS, YS, fracture strength (FS), and percent elongation of the specimens. Hardness was also determined.

3.4.1 Tensile Testing

Tensile testing was conducted according to the parameters listed in the AMS 4999 specification and the results are listed in Table 3.1. Specimens labeled with a "P" indicate that specimen was grown on pins instead of the heated steel start plate. Figure 3.14 compares the average values of some of the mechanical properties for each of the three build orientations.

Table 3.1: Tensile Mechanical Properties of Ti-6Al-4V Specimens Fabricated Using the Arcam EBM Process

Specimens	Cross-Sectional Area (in ²)	UTS (ksi)	0.2% Yield Strength (ksi)	%Elongation	Fracture Strength (ksi)
XY1	0.0607	150.74	134.442	9.19	149.22
XY2	0.0588	152.02	138.819	6.68	151.40
XY3	0.0643	152.39	145.905	6.85	149.73
XY6	0.0623	153.01	143.454	8.49	152.61
XY7	0.0598	154.18	143.051	7.45	152.42
XY8	0.0605	167.80	160.548	17.03	160.71
XYP1	0.0571	170.35	161.522	14.13	166.10
XYP2	0.0620	153.52	144.970	16.27	148.82
Average	0.0607	156.75	146.59	10.76	153.88
StDev	0.0022	7.71	9.65	4.34	6.21
XZ1	0.0620	158.61	152.11	7.56	158.51
XZ3	0.0630	160.94	155.89	8.23	160.65
XZ6	0.0605	157.02	152.91	12.32	152.81
XZ7	0.0627	150.72	135.72	4.86	149.73
XZ8	0.0617	157.59	153.40	15.73	150.85
XZ9	0.0610	156.15	146.38	3.60	143.01
XZ10	0.0617	156.79	151.09	10.19	155.29
Average	0.0618	156.83	149.64	8.93	152.98
StDev	0.0009	3.12	6.79	4.22	5.91
YZ1	0.0603	152.05	141.45	17.24	136.56
YZ2	0.0620	152.80	141.96	13.44	149.16
YZ3	0.0610	154.57	139.34	14.75	146.28
YZ6	0.0620	153.75	133.06	16.86	138.43
YZ7	0.0618	158.36	137.16	16.01	151.03
YZ8	0.0625	153.90	143.46	13.13	149.63
YZP2	0.0608	140.40	134.38	12.54	138.17
YZP3	0.0605	154.44	138.25	16.16	145.50
Average	0.0613	152.54	138.63	15.02	144.34
StDev	0.0008	5.24	3.67	1.81	5.79

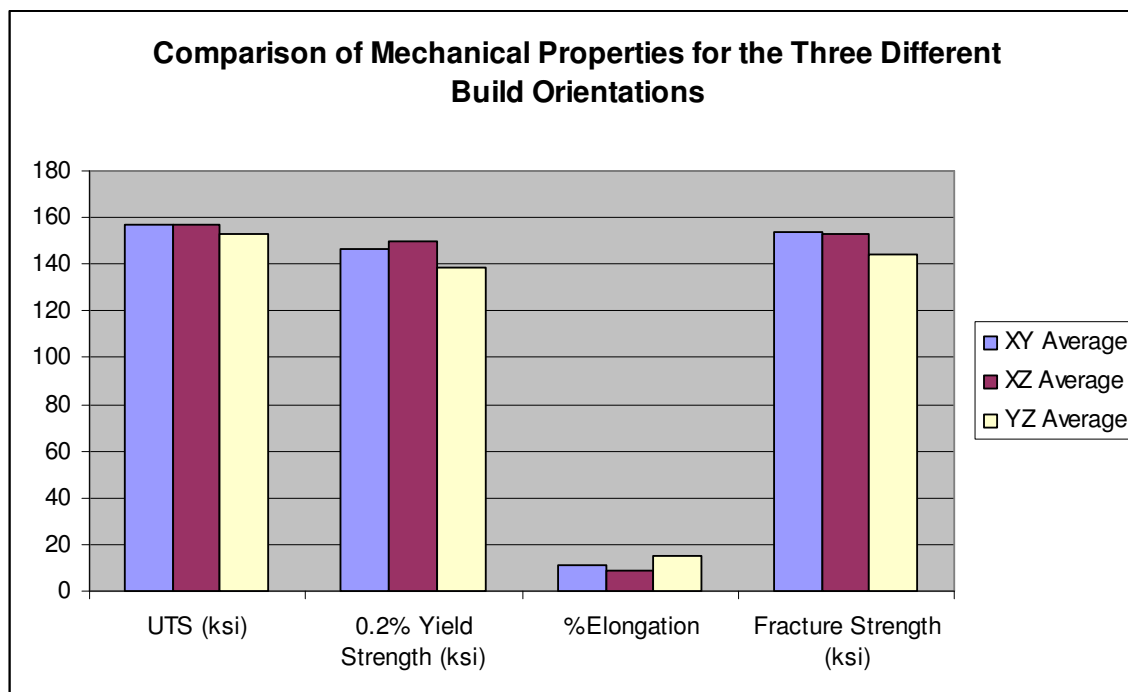


Figure 3.14: Comparison of Average Tensile Mechanical Properties for the Three Different Build Orientations

As shown in the above table, specimens built in the XZ orientation had the highest average UTS and YS values, however the values for the XY specimens were very similar. Although, the YZ specimens were the weakest of the build orientations, they did have the highest percent elongation meaning they were the most ductile. The XZ specimens had the lowest ductility of the samples. This low ductility is likely linked to the columnar grains that are aligned parallel to the tensile axis for the XZ build orientation. This same relationship may also be the cause of the XZ specimens' higher strength.

The samples that grew on pins (build orientations D and E from Figure 3.3) were devised as a way to test the effect of the difference in the coefficients of thermal expansion (CTE) between the titanium alloy and the steel start plate. It was proposed that this variation of the

CTE could lead to added stresses in the part, however, Table 3.1 shows that the samples grown on pins displayed properties that, on average, were the same as the samples grown on the steel start plate.

In order to validate the Arcam EBM process as an acceptable alternative to conventional fabrication methods, the mechanical properties of Ti-6Al-4V alloy samples fabricated using the Arcam EBM process were compared to Ti-6Al-4V samples fabricated by other methods such as various casting, forging, and laser deposition procedures. These procedures are all outlined in different Aerospace Material Specifications (AMS). Table 3.2 shows the comparison of the average mechanical property values of the Arcam specimens compared to the minimum allowable values of those fabricated according to various AMS procedures. Figure 3.15 displays this comparison more clearly.

Table 3.2: Comparison of the Average Values of Selected Mechanical Tensile Test Parameters from Arcam EBM Fabricated Ti-6Al-4V Alloys to Various Aerospace Material Specifications for the Ti-6Al-4V Alloys Produced Using Already Established Methods

	Process	UTS (ksi)	Yield Strength (ksi)	%Elongation	Fracture Strength (ksi)
XY Average	Arcam EBM	156.75	146.59	10.76	153.88
XZ Average	Arcam EBM	156.83	149.64	8.93	152.98
YZ Average	Arcam EBM	152.54	138.63	15.02	144.34
AMS-T 9047¹	Forged, Square, <.5 in ²	165.00	155.00	10.00	
AMS-T 81915²	Cast	125.00	115.00	8.00	
AMS 4999³: (x direction)	Energy Beam Process	130.00	116.00	4.00	
(y&z direction)	Energy Beam Process	122.00	108.00	4.00	
AMS 4985C⁴: (separately- cast)	Cast	130.00	120.00	6.00	
(integrally- cast, designated areas)	Cast	130.00	120.00	6.00	
(integrally- cast, nondesignated areas)	Cast	125.00	108.00	4.50	

1. AMS-T 9047: Titanium and Titanium Alloys, Bars (Rolled or Forged) and Reforging Stock, Aircraft Quality
2. AMS-T 81915: Titanium and Titanium-Alloy Castings, Investment
3. AMS 4999: Titanium Alloy Laser Deposited Products 6Al-4V Annealed
4. AMS 4985C: Titanium Alloy, Investment Castings 6Al-4V 130 UTS, 120 YS, 6% EL Hot Isostatically Pressed Anneal Optional or When Specified

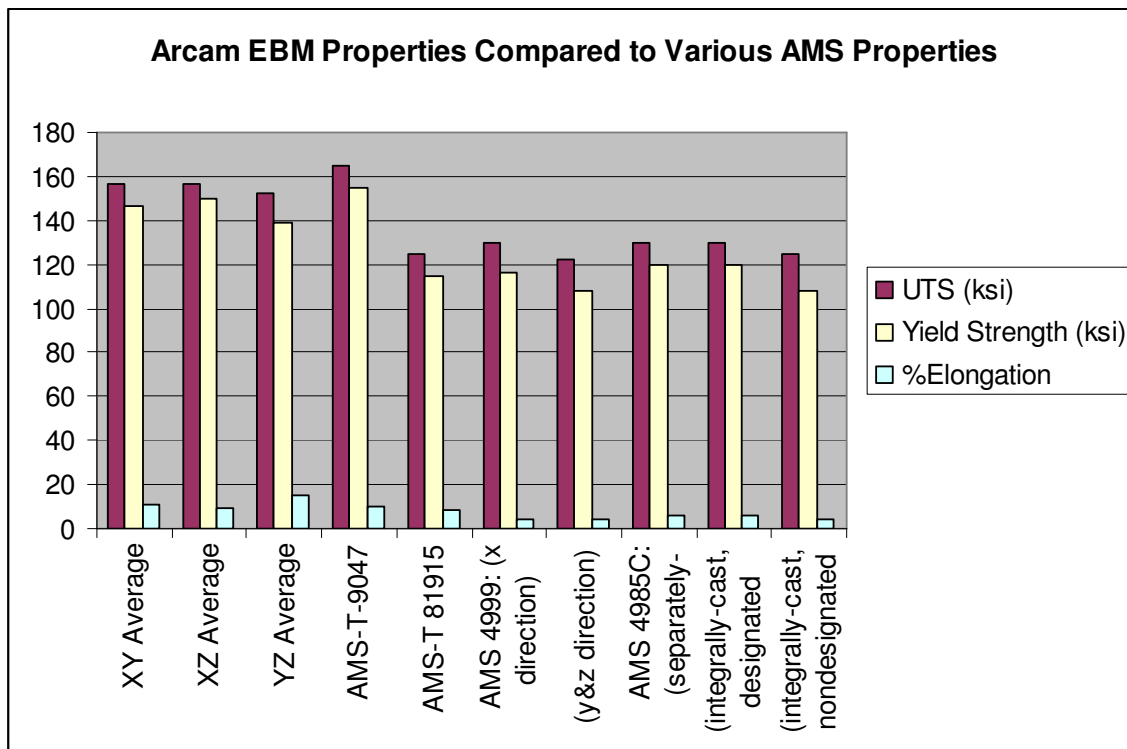


Figure 3.15: Comparison of the Average Values of Selected Mechanical Tensile Test Parameters from Arcam EBM Fabricated Ti-6Al-4V Alloys to Various Aerospace Material Specifications for the Ti-6Al-4V Alloys Produced Using Already Established Methods

From Table 3.2 and Figure 3.15, it is found that the Arcam EBM process exceeds all the minimum requirements given in the cast and laser deposition specifications. The YS and UTS for the forged specification (AMS-T 9047), however, are higher than those found for the Arcam EBM samples. With the exception of the XZ samples, the Arcam EBM samples meet the percent elongation requirement for the forged specification. Based on the results of this data, it appears that the alloy samples produced by the Arcam EBM process in this study generally meet or exceed the required mechanical properties for alloys that are produced according to the cast and laser deposition specifications.

3.4.2 Hardness

Another manner of validating Ti-6Al-4V specimens produced by the Arcam EBM process is to compare their hardness values to that of Ti-6Al-4V alloys produced by previously established methods. Table 3.3 shows the average hardness values of the Arcam EBM produced samples, from all three build orientations on all three surface planes, compared to the hardness of a typical Ti-6Al-4V alloy.

Table 3.3: Average Hardness Values for Arcam EBM Produced Ti-6Al-4V Specimens Compared to a Typical Ti-6Al-4V Alloy

Hardness Test			
Specimen	Plane	Average Hardness (Rockwell C)	Standard Deviation
XY	Face	39.0	1.31
XY	Edge	37.0	0.60
XY	Cross-Section	36.6	1.74
YZ	Face	35.6	0.99
YZ	Edge	36.3	1.20
YZ	Cross-Section	37.1	0.77
XZ	Face	35.5	0.00
XZ	Edge	36.7	1.15
XZ	Cross-Section	38.2	1.04
Typical Ti-6Al-4V Alloy		36.0 ¹	

1: Source-Titanium Information Group

As shown in this table, the average hardness values for Arcam EBM produced Ti-6Al-4V samples are essentially the same as that of Ti-6Al-4V alloys produced by previously established methods.

3.4.3 Fracture Toughness

In addition to tensile and hardness testing, Ti-6Al-4V Arcam EBM fabricated samples also underwent fracture toughness testing. The fracture toughness tests were carried out according to the ASTM E399-90 standard⁽⁴⁾. The samples were tested using a horizontal build orientation (XY) and a vertical build orientation (XZ). The results of the fracture toughness tests are shown in Figure 3.16.

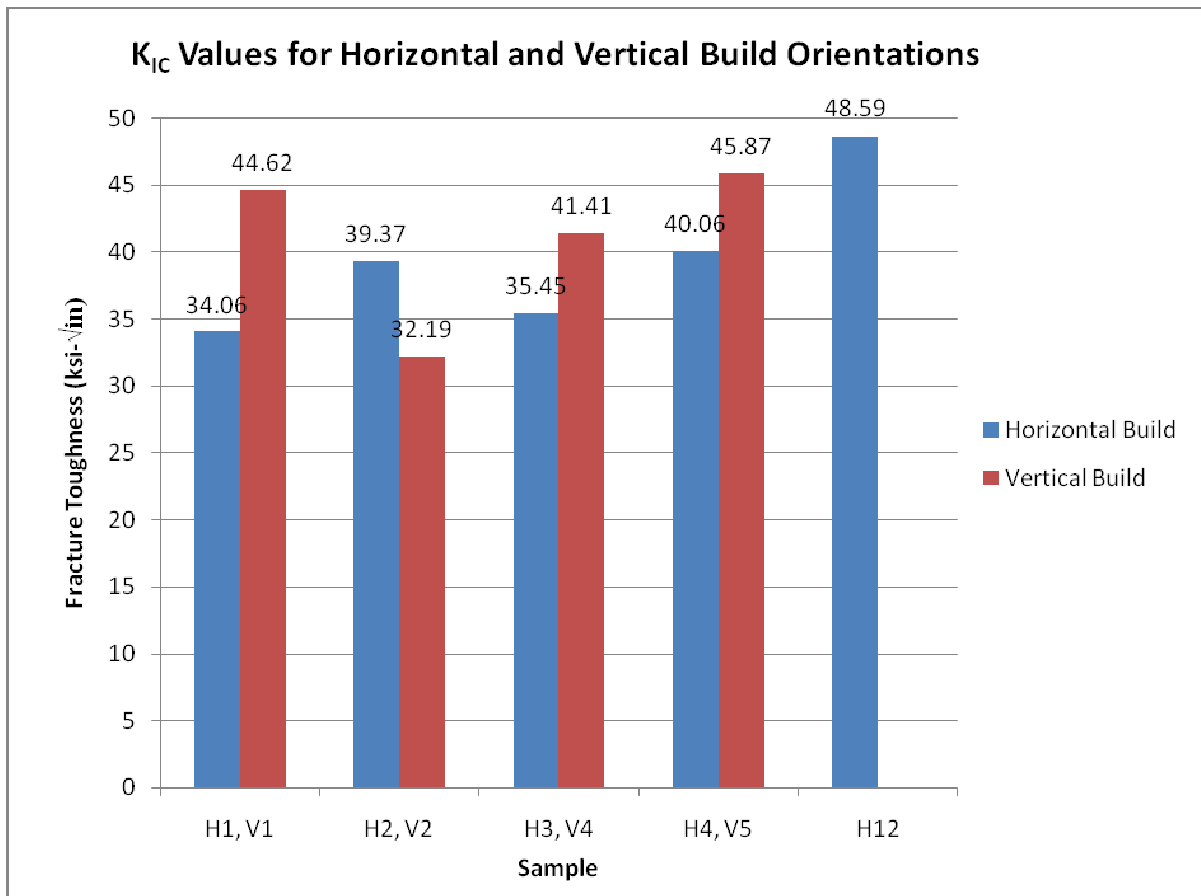


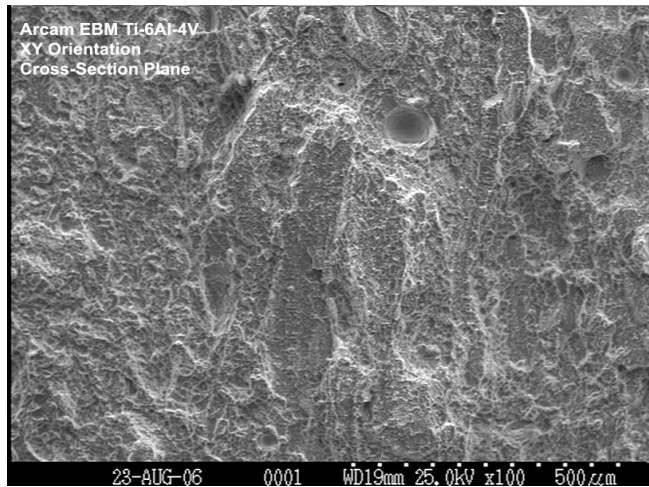
Figure 3.16: Fracture Toughness Values for Horizontally and Vertically Oriented Arcam EBM Fabricated Ti-6Al-4V Specimens

From the figure, it is found that the average determined fracture toughness value is 39.51 ksi-in^{1/2} for the horizontal specimens and 41.02 ksi-in^{1/2} for the vertical specimens.

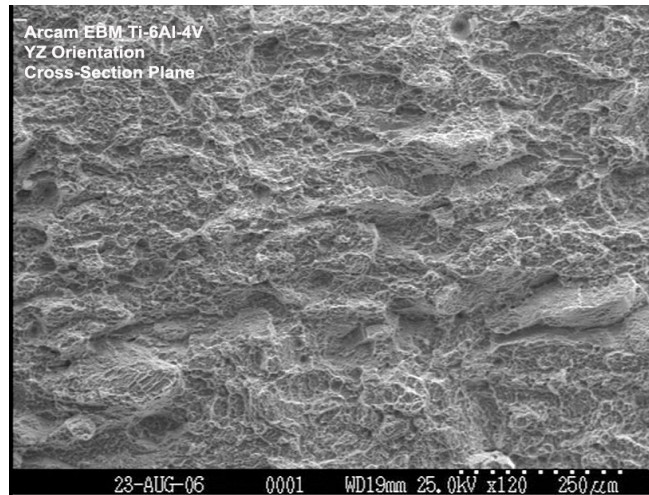
The typical fracture toughness values for traditionally fabricated Ti-6Al-4V alloys range from the upper 30's to lower 90's ksi-in^{1/2(5)}. One possible explanation for the rather low fracture toughness values for these samples is the fact that powder used was made using a plasma rotating electrode process (PREP). This process generally produces a less desirable powder morphology, which could affect the material properties (see Section 3.6.3). In order to obtain a more accurate understanding for the fracture toughness values of Arcam EBM produced Ti-6Al-4V specimens, more samples will need to be tested.

3.5 Fractography

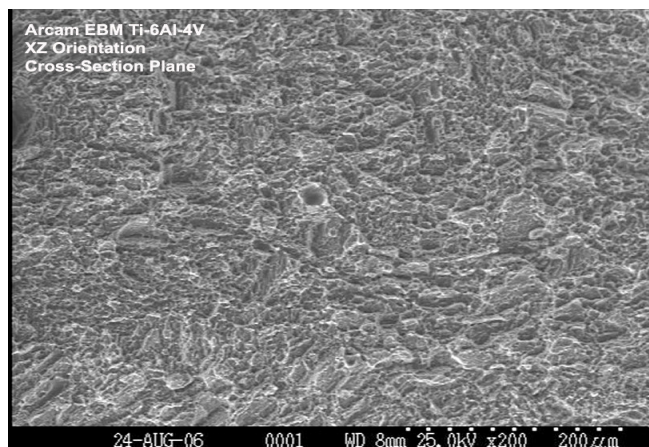
The fracture surfaces of the Arcam EBM produced tensile specimens were observed using a SEM in order to understand their fracture behavior and the correlation between the samples' microstructures and its tensile mechanical properties. Overall, the fracture surfaces appeared to have a moderately ductile nature, as indicated by the present of dimples and microvoids. The observance of slight necking in the specimens along with areas of plastic deformation in the stress-strain curves further validates this claim. Fracture bands were also observed along the surfaces, and appeared to coincide with the columnar grains found in the microstructure. This relationship is shown in the SEM images in Figure 3.16



(A)



(B)



(C)

Figure 3.17: SEM Fractographs of Arcam EBM produced Ti-6Al-4V Tensile Specimens

Figure 3.17 (A) shows a fracture surface of a XY oriented specimen with the face plane aligned along the top and bottom edges of the image. The fracture bands in this image run normal to this face plane direction, which is the same direction the columnar grains run for this build orientation. Figure 3.17 (B) shows a fracture surface of a YZ oriented specimen with the face plane aligned along the top and bottom edges of the image, as was the case in Figure 3.17 (A). The fracture bands in this image run parallel to this face plane direction, which is the same direction the columnar grains run for this build orientation. Figure 3.17 (C) shows a fracture surface of a XZ oriented specimen with the face plane aligned along the same direction as in the previous two images. This image does not appear to display any fracture bands, which would correspond to the fact that the columnar grains for this build orientation run along the tensile axis, so only the cross-sections of the columnar grains would be shown.

The images above provide evidence to state that there is a direct correlation between the fracture bands and the columnar grains in these Arcam EBM produced samples. Thus, considering that the XZ oriented samples were stronger than the XY and YZ oriented samples, the columnar grains must be a factor in providing strength to these specimens. Since the columnar grains remained intact on the fracture surfaces, it is likely that the cracks propagated intergranularly. Intergranular crack propagation is also supported by the fact that all of the fracture surfaces contained shear lips.

3.6 Improvement of Microstructural and Mechanical Properties

Although the mechanical data discussed previously shows the Arcam EBM process as a favorable alternative to laser deposition and casting techniques, it is still of interest to improve the mechanical properties of specimens produced by the Arcam EBM process so that they meet the specifications for forged Ti-6Al-4V alloys as mentioned in AMS-T 9047. Improvement of the mechanical properties can be achieved by refining the microstructure of the material and reducing contamination. Some of the proposed methods for improvement are as follows: varying the raster pattern and other parameters of the electron beam, hot isostatic pressing (HIP) and/or heat treating at various times and temperatures, and varying the morphologies and sizes of the powder alloy.

3.6.1 Varying the Process Parameters of the Arcam EBM Machine

One of the simplest ways to try and improve upon the properties of Ti-6Al-4V specimens produced using the Arcam EBM process is to alter the parameters of the electron beam. Power, beam velocity, traverse velocity, and raster pattern are all parameters that are controllable on the Arcam EBM machine. There is little information available on the effects of process parameters on mechanical properties for the Arcam EBM process. However, research has been conducted on the effect of process parameters for a similar process called Laser Engineered Net Shaping (Lens). LENS is a laser deposition process in which, like the Arcam EBM process, metal parts are fabricated layer by layer directly from CAD models. A study was conducted in which the power and traverse velocity of the laser beam was altered and the effects of these alterations on the properties of H13 tool steel was observed⁽⁶⁾. By

changing the power and velocity of the laser, the deposition energy was altered, which was found to affect the strength and ductility properties of the alloy. H13 tool steel is susceptible to the Hall-Petch effect, which states that microstructures with finer grain sizes result in higher yield strengths. A low deposition energy, characterized by low power (200 W) or high traverse velocity (9.31 mm/s), allowed the molten pool to quickly solidify leading to a finer microstructure with smaller grains⁽³⁾ and therefore high yield and ultimate tensile strength values. A high deposition energy, characterized by high power (300 W) and/or slow traverse velocity (5.92 mm/s), produced parts with a coarser microstructure with larger grains⁽³⁾ and high ductility; thus the highest strength and ductility values cannot be attained simultaneously.

This same study also observed how laser beam power affected the molten pool size in the alloy, which in turn affects the thermal gradient across the molten pool and into the bulk material. It was found that the size of the molten pool increased with power up to 275 W. Using a power above 275 W caused the pool temperature to increase, but did not significantly change the size of the molten pool. Since the molten pool size remained constant, the heat dispersed into the bulk resulting in a lower cooling rate after solidification.

Research has also been conducted examining the effect of electron beam velocity on the densification of H13 tool steel fabricated using the Arcam EBM process⁽⁷⁾. In this study, electron beam velocities of 2,500 mm/sec, 2,000 mm/sec, 1,500 mm/sec, and 1,000 mm/sec were tested and their effect on the respective samples' densifications was tested.

The results of this experiment indicated that complete densification occurred in the samples using beam velocities of 1,500 mm/sec and slower. The higher beam velocity samples appeared to be very loosely bonded and therefore not suitable for usable parts.

Another parameter that is controllable on the Arcam EBM machine is the raster pattern. The raster, or hatch, pattern is the direction and spacing in which the electron beam moves during part fabrication. Altering this pattern can change the temperature gradients, cooling rates, and melt flow of the material; all of which can impact the microstructural and mechanical properties of fabricated parts. All the samples used in this work were made with the electron beam changing 90° in direction between each layer. This raster pattern is shown in Figure 3.18.

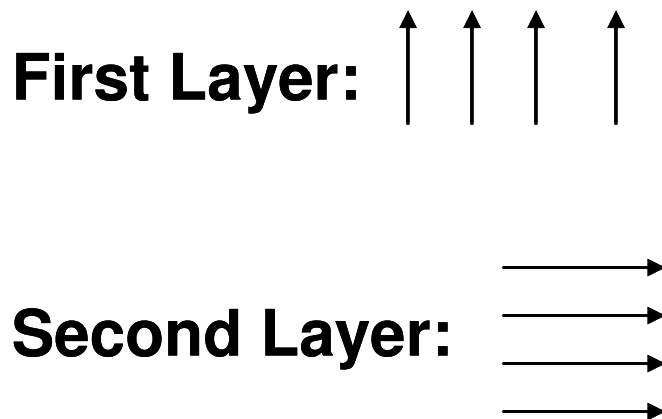


Figure 3.18: Raster pattern used in Arcam EBM process

The direction of the electron beam can be changed between layers, as shown above, or between passes within the same layer, both of which can affect the microstructure. To understand how varying the raster pattern affects the temperature gradients and, in turn, the heat flow, a thermocouple could be inserted directly into the powder during fabrication. This

technique was done in a previous study investigating the thermal history during LENS processing⁽⁶⁾. In this study, in-situ temperature readings were taken for twenty deposition layers during the fabrication of H13 tool steel. The study revealed peaks in the temperature each time the laser passed over or near the thermocouple, from the initial layer to subsequent layer depositions. During the first layer deposition the temperature peaked at 1500°C and quickly cooled to about 150°C. Each subsequent pass reheated the previous layers so that after five layers were deposited, the initial layer still reached temperatures up to 900°C. After thirteen layers were deposited, the thermocouple nominally read 500°C. Due to the complex thermal cycling associated with the LENS process, the material properties of the samples are affected much in the same way as they would be from tempering or aging. Conducting a similar study for the Arcam EBM process using various raster patterns would give insight as to how changing the raster patterns affect the microstructure and material properties of a part.

3.6.2 HIP and/or Heat Treating at Various Times and Temperatures

Hot isostatic pressing and/or heat treating Ti-6Al-4V alloys is a common way to alter the microstructure and mechanical properties of parts produced by traditional fabrication techniques. Titanium alloys can be heat treated in order to: reduce residual stresses produced during fabrication (stress relieving); produce the most favorable combination of ductility, machinability, and structural and dimensional stability (annealing); increase strength (solution treating and aging); and improve special properties such as fatigue strength, fracture toughness, and high temperature creep strength⁽⁸⁾.

Stress relieving Ti-6Al-4V alloys reduce the undesirable residual stresses resulting from: nonuniform hot forging or deformation from cold forming and straightening, asymmetric machining of forgings or plates, and welding and cooling of castings⁽⁸⁾. Removing these stresses helps maintain shape stability and prevents undesired conditions. Stress relieving of Ti-6Al-4V alloys is done at temperatures between 480-650°C for 1 to 4 hours as stated in AMS-H-81200A⁽⁹⁾. After stress relieving, the alloys can be cooled by either air or furnace cooling. Stress relieving parts fabricated using the Arcam EBM process may help relieve residual stresses due to part formation and shaping.

Annealing Ti-6Al-4V alloys is mainly done in order to improve fracture toughness, dimensional and thermal stability, and ductility at room temperature⁽⁸⁾. Annealing titanium alloys usually improves some properties at the expense of others, so the annealing cycle must be selected in accordance with the desired property traits. There are several common types of annealing treatments, but recrystallization annealing provides the optimal combination of improvement in fracture toughness without significant loss in strength. This process is done by heating the alloy into the upper range of the α - β region, held for a period of time, and then slowly cooled. AMS-H-81200A recommends recrystallization annealing at temperatures between 968-986°C, holding for 1 to 4 hours, air cooling or slower, reheating between 705-760°C for 1 to 2 hours and then air cooling again⁽⁹⁾. Arcam EBM fabricated Ti-6Al-4V alloys could undergo this process in order to improve their fracture toughness, while still maintaining their strength.

Solution treating and aging Ti-6Al-4V alloys can result in a wide range of strength values. Heating a Ti-6Al-4V alloy to the solution treating temperature leads to a higher ratio of β phase, which can be maintained by quenching. Subsequent aging causes the unstable β phase to decompose, resulting in high strength. Solution treating is usually done high in the α - β region in order to obtain high strength with sufficient ductility. The solution heat treating schedule listed in AMS-H-81200A is heating between 900-970°C for 20 to 120 minutes, followed by water quenching⁽⁹⁾. Water quenching provides the cooling rate necessary to prevent the β phase from decomposing and allows for the maximum response to aging. Aging causes the supersaturated β phase left over from quenching to decompose. The aging schedule listed in AMS-H-81200A is heating between 480-690°C for 2 to 8 hours, depending on the desired strength level. Like the previous heat treatments, solution treating and aging Ti-6Al-4V alloys fabricated using the Arcam EBM process can help provide the optimal combination of strength, ductility, and toughness.

When heat treating Ti-6Al-4V alloys, it is important to consider the effects of contamination. Heat treating must be done in a vacuum furnace or an inert atmosphere in order to prevent oxidation of the alloy, which can produce a brittle surface layer. Heat treating in a vacuum furnace or inert atmosphere also, more importantly, prevents having a high concentration of hydrogen (above 125 to 200 ppm), which can lead to premature failure of a Ti-6Al-4V part⁽⁸⁾.

HIP Ti-6Al-4V parts is also a relatively common way to increase some of the material properties. HIP involves exposing parts to elevated temperatures and pressures, which

results in the removal of internal voids and helps create strong metallurgical bonds throughout the material⁽¹⁰⁾. The HIP part becomes almost 100% dense and homogeneous with a uniformly fine grain size. Since HIP parts have reduced porosity, their mechanical properties, such as fatigue strength, and workability are improved. AMS 4992 suggests that Ti-6Al-4V parts be HIP in an inert atmosphere of 14.5 ksi or greater within the temperature ranges of 899 to 954°C, held for 2 to 4 hours, and cooled under inert atmosphere to below 427°C⁽¹¹⁾. Subjecting Arcam EBM produced Ti-6Al-4V parts to this treatment could aid in reducing some of the observed porosity in the parts and therefore, improving the mechanical properties.

3.6.3 Varying the Morphologies and Sizes of the Powder Alloy

One of the most important aspects of the Arcam EBM process is how well the powder packs in the Arcam chamber. Packing density is crucial in allowing adequate electrical and thermal conductivity throughout the powder. Inadequate conductivity can cause the powder to develop a buildup of negative charge, which causes the powder to repel against the electron beam, thereby ruining the run. The powder density also plays a role in how well the powder melts and flows during a run. Powder density is a result of the size and morphologies of the powder itself. As mentioned in Chapter 3.2, all the Ti-6Al-4V powder used in this research was gas atomized and ranged from 44 to 149 μm in size. One obvious way to improve the packing density of the powder would be to use powder that varies in size. This would allow the smaller powder to fill in the voids created by the larger powder. Changing the shape of

the powder could also increase its packing density. Thin, elongated “flake-shaped” powder has the potential to pack more densely than powder of a spherical shape.

Currently, another method of powder production being used in conjunction with the Arcam EBM process is plasma rotating electrode process (PREP). This process involves creating the desired alloy in the form of a rotating bar that is arced with plasma gas. The bar is heated by the plasma and the molten metal is centrifugally flung off of the bar, cooled down, and collected as powder⁽¹²⁾. The shape of the powder collected, however, is spherical and ranges from 100 to 300 μm in size, thereby making it less desirable than gas atomized powder due to its reduced packing density.

References

1. R.M. German. *Powder Metallurgy Science: Second Edition*. Metal Powder Industries Federation. Princeton, NJ. 1994
2. R. Boyer. *Metals Handbook Ninth Edition: Volume 9 Metallography and Microstructures*. American Society for Metals. USA. 1985.
3. P. A. Kobryn et al. *Microstructure and Texture Evolution During Solidification Processing of Ti-6Al-4V*. Journal of Materials Processing Technology. 2003.
4. ASTM E399-90. *Standard Test Method for Plane-Strain Fracture Toughness of Metallic Materials*. 1997.
5. www.matweb.com
6. M. L. Griffith et al. *Understanding the Microstructure and Properties of Components Fabricated by Laser Engineered Net Shaping (LENS)*. Sandia National Laboratories. Albuquerque, NM.
7. D. Cormier et al. *Optimization of Electron Beam Melting Process*. IIE Annual Conference. 09C Rapid Prototyping III. 2004.
8. D. Betner et al. *Metals Handbook Ninth Edition: Volume 3 Properties and Selection: Stainless Steels, Tool Materials and Special-Purpose Metals*. American Society for Metals. USA. 1980.
9. AMS-H-81200A. *Heat Treatment of Titanium and Titanium Alloys*. April 2001.
10. S. Mussman et al. *Materials World*. Volume 7. Number 11. Pages 677-678. November 1999.
11. AMS 4992. *Castings, Structural Investment, Titanium Alloy 6Al-4V Hot Isostatically Pressed*. October 2002.
12. *Titanium Powder Metallurgy*. Data Sheet No 18. Titanium Information Group. February 2006.

Chapter 4: Conclusion

With the increasing market for rapid manufactured metal alloy parts, new fabrication technologies must be established that are able to meet this demand. The Arcam EBM process allows for the rapid manufacturing of metal alloy parts with low tooling costs and essentially no material wasted as scrap. Parts having intricate dimensions and geometries are able to be produced with little or no need for machining. With its unique capabilities, the Arcam EBM process has potential applications in various markets, such as replacing parts on military aircraft, complex engine designs, and medical implants. In order to establish this technology as a viable alternative to traditional metal alloy manufacturing techniques, certain material properties and characterization on parts produced using the Arcam EBM process must be examined. The purpose of this research was to analyze the mechanical and microstructural properties of Ti-6Al-4V alloys produced using the Arcam EBM process in an effort to determine whether or not this process is an acceptable alternative to traditional manufacturing methods.

Mechanical testing was conducted on Arcam EBM produced Ti-6Al-4V samples in accordance with various AMS and ASTM standards and specifications. Microscopy was also carried out in order to evaluate the microstructure of the samples. The relationship between the mechanical properties and the microstructural properties of the samples was established. The data collected from these samples was compared to the properties of Ti-6Al-4V alloys fabricated using laser deposition, casting, and forging techniques. It was found that, in general, the properties of Arcam EBM produced Ti-6Al-4V alloys meet the

minimum material property requirement given in these more traditional fabrication processes, and is therefore, an acceptable fabrication process for Ti-6Al-4V alloys.

Suggestions on ways to improve the properties of Arcam EBM produced Ti-6Al-4V alloys by altering the Arcam EBM parameters and using post fabrication heat treatment were given in hopes to further establish this technology. Future work will consist in trying to produce parts made from aluminum alloys in an effort to establish the Arcam EBM process as an acceptable means of aluminum alloy fabrication as well.